The role of topography on projected rainfall change in mid-latitude mountain regions

Michael R. Grose, Jozef Syktus, Marcus Thatcher, Jason P. Evans, Fei Ji, Tony Rafter & Tom Remenyi

Climate Dynamics
Observational, Theoretical and Computational Research on the Climate System

ISSN 0930-7575

Clim Dyn
DOI 10.1007/s00382-019-04736-x

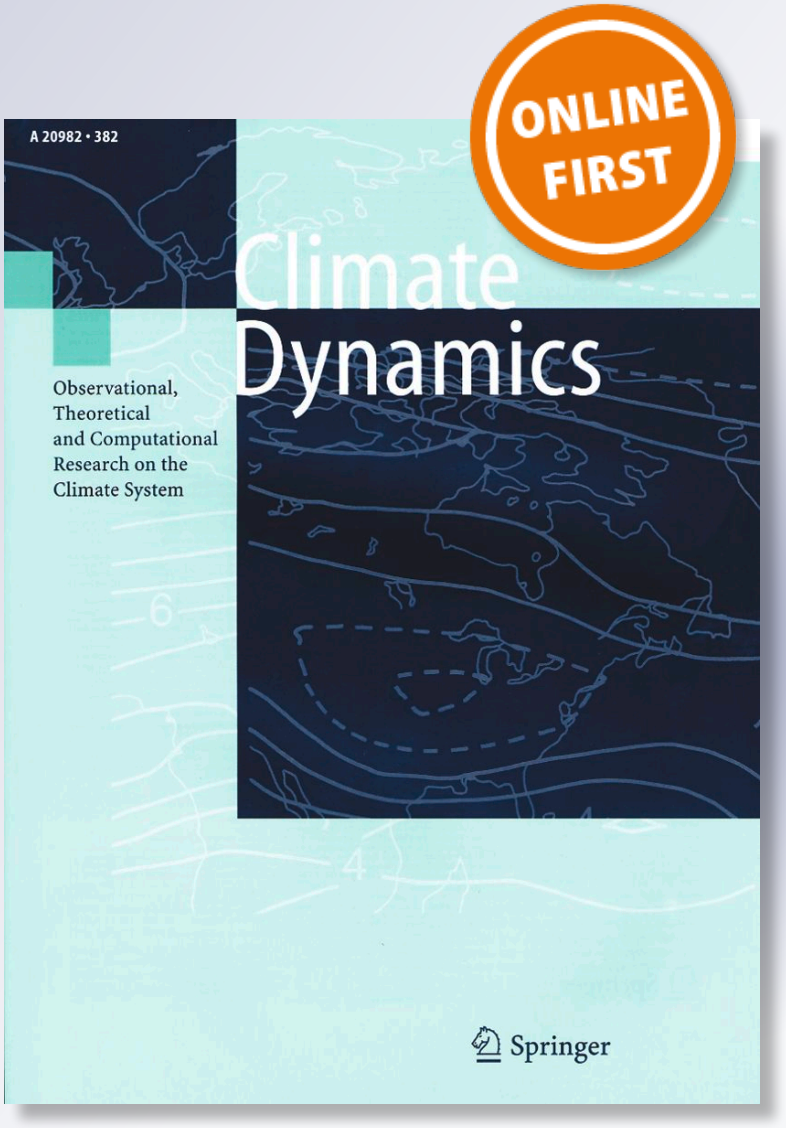

Springer

Climate Dynamics
https://doi.org/10.1007/s00382-019-04736-x

The role of topography on projected rainfall change in mid-latitude mountain regions

Michael R. Grose[1] · Jozef Syktus[3] · Marcus Thatcher[2] · Jason P. Evans[4] · Fei Ji[5] · Tony Rafter[2] · Tom Remenyi[6]

Received: 30 April 2018 / Accepted: 16 March 2019

Abstract

Change to precipitation in a warming climate holds many implications for water management into the future, and an enhancement of a precipitation decrease or increase on or around mountains would have numerous impacts. Here, an intermediate resolution regional climate model (RCM) ensemble projects enhanced precipitation decrease on the windward slopes of over many mid-latitude mountains in winter, consistent with theory and model studies of idealised mountain ranges. This ensemble projects that an increase in convective rainfall determines the sign of total rainfall change in many regions in summer, only some of which are on or near mountains such as the European Alps. These same projected changes are present in inland slopes of the Australian Alps compared to surrounding regions as simulated by three RCM ensembles (the intermediate resolution and two high resolution ensembles), which agree on an enhanced precipitation decrease on the windward slopes in winter and spring, as well as an enhanced precipitation increase in summer driven by an increase in convective rainfall. The ensembles disagree on an enhanced precipitation decrease in autumn. The results represent regional-scale added value in the climate change signal of projections from high resolution models in cooler seasons, but suggest that the specific model components such as convection schemes strongly influence projections of summer rainfall change. Confidence in the simulation of change in convective rainfall, or convection-permitting modelling may be needed to raise confidence in summer rainfall projections over mountains.

Keywords Regional climate models · Added value · Rainfall · Climate change

1 Introduction

Changes to regional rainfall due to anthropogenic climate change has implications for stream flows, water resources, hydropower generation, tourism, flooding, agriculture and natural systems into the future, including over mountain ranges (Beniston and Stoffel 2014). Topography is likely to affect the regional rainfall change over mountain ranges, including those in the mid-latitude band. To understand the likely projected rainfall change over these mid-latitude mountain ranges, and assess the certainty in the projection, it is useful to assess the change expected from physical theory, and how well it aligns with projections using models that can resolve mountains.

A warming climate drives changes to precipitation through changes in thermodynamics as well as circulation, affecting all forms of precipitation including stratiform rainfall, convective rainfall, snow and graupel (Collins et al. 2013). In addition, warming affects the temporal distribution of rainfall, typically including an increase in extremes (Held

Electronic supplementary material The online version of this article (https://doi.org/10.1007/s00382-019-04736-x) contains supplementary material, which is available to authorized users.

✉ Michael R. Grose
Michael.Grose@csiro.au

1 CSIRO Oceans and Atmosphere, Hobart, Australia

2 CSIRO Oceans and Atmosphere, Melbourne, Australia

3 Global Change Institute, The University of Queensland, Brisbane, Australia

4 Climate Change Research Centre and ARC Centre of Excellence for Climate Extremes, University of New South Wales, Kensington, Australia

5 New South Wales Office of Environment and Heritage, Sydney, Australia

6 Antarctic Climate and Ecosystems Cooperative Research Centre, Hobart, Australia

Published online: 22 March 2019

and Soden 2006; Chou et al. 2012). Effects from orography affect rainfall change, such as the formation of mountain barrier jets (Dezfuli et al. 2017) shadowing from topographic barriers and orographic convection. Feedbacks such as those involving snow and ice cover typically lead to enhanced projected warming over mountains (Rangwala and Miller 2012; Minder et al. 2018), and this may influence change in total precipitation (Im et al. 2010). The shift from precipitation falling as snow to rain causes a deepening of rain shadows and affects the spatial distribution of water resources, floods and landslides (Pavelsky et al. 2012). The balance of all these factors determines overall projected change in precipitation over any mountain region.

Looking first at the cool seasons, the mid-latitudes are projected become drier due to changes in the predominantly westerly circulation and a reduction in stratiform rainfall (Collins et al. 2013). So a key question is whether this reduction in stratiform rainfall is enhanced or ameliorated over mountain ranges compared to low elevation. In simulations of simplified low-elevation mid-latitude mountains, stratiform rainfall decreases on windward slopes in 40–50 °N, despite an increase in extreme rainfalls and water vapour fluxes (Shi and Durran 2014). This study found that the overall rainfall decrease can be explained by a simple balance between an increase in precipitation of 4–5% K^{-1} following the effect of the Clausius–Clapeyron relation on rainfall (Held and Soden 2006), countered by a decrease in the westerly wind speed related to the movement of the storm track, and a decrease in saturated vertical displacement related to the relative humidity aloft during rainy events. This study also found strong north–south gradients in the sensitivity of rainfall change to temperature, so simulating fine scale changes over realistic mountains will depend on the accuracy of large-scale flows. The shape and size of mountain ranges is important in that they affect the change in the drying ratio (the fraction of impinging water vapour falling as precipitation), and several other factors (Eidhammer et al. 2018). If this rainfall change is reflected in simulations of real mid-latitude mountain ranges, we expect an enhanced drying on windward slopes especially the poleward extents of the ranges.

Turning to summer, changes in convective rainfall with a warming climate must also be considered. As temperature increases, variables such as low-level potential instability and convective available potential energy (CAPE) increase. Mountains influence convection through surface heating forcing convection and destabilising the overlying mid-tropospheric layers, and also through inducing mesoscale circulation and convergence (Giorgi et al. 1997). Cannon et al. (2012) suggest that changes in embedded convection due to warmer, less stable upstream flows would lead to greater precipitation efficiency and enhanced drying ratios, with moderate precipitation increases over wide ridges, but significantly more modified orographic precipitation over narrow ridges. This is likely to be important in summer in mid-latitude mountain ranges, and could be reflected in enhanced rainfall increase on mountain tops.

High-resolution regional climate models (RCM), can more finely resolve the relevant regional processes and topography than coarse global climate models (GCMs), including the effect of topography. The extra regional detail in the simulation of the current climate is known as 'added value'. Similarly, extra regional detail or 'added value' can be found in the projected climate change signal, also noted as 'downscaling signal' using the framework of Di Luca et al. (2012). In relation to mid-latitude mountain ranges, notable regional-scale added value has been found through fine resolution modelling in the European Alps (Torma et al. 2015). Downscaling revealed a projected increase in rainfall at high elevation in Boreal Summer (JJA), in contrast to the drying of the surrounding region (Kotlarski et al. 2012), and the projected changes to convective rainfall tips the balance and determines this sign of change (Giorgi et al. 2016). A topographic dependence has been found in changes to dry spells, wet spells and extremes in the European Alps (Gao et al. 2006). At higher elevation but below mountain peaks in summer there is a projected decrease in rainfall, including a decrease in the number of wet days and wet day intensity, and an increase in the number of multi-day dry spells (Fischer et al. 2015). Increases in convective rainfall leading to an increase in total rainfall over mountains in the warmer seasons, in contrast to general rainfall decrease in the cool season driven by changes to other rainfall types, has been found not only in the European Alps (Giorgi et al. 2016), but in the American Rocky Mountains (Leung and Ghan 1999).

Here we look at the projected change in rainfall over mid-latitude mountain ranges (25–50° latitude) in transient climate change model simulations with realistic topography, and examine the patterns of enhanced drying in winter and enhanced rainfall increase in summer. We look at a few example cases in this latitude band, with a particular focus on the Australian Alps as a case of a mountain range with a restricted, seasonal snow cover and relatively low elevation (up to around 2200 m compared to 4800 m in the European Alps). This case is chosen reveal where the processes may be more subtle or marginal. Previous work has shown that total precipitation is significantly declining on the western and high slopes but not the eastern slopes, likely due to changes in the westerly circulation, and expressed through a reduction in intensity of rainfall events (Fiddes and Pezza 2015; Fiddes et al. 2015). Previous RCM studies projected enhanced drying at higher elevation compared to the general drying in the Australian Alps region annually and in most seasons (Harris et al. 2016; Olson et al. 2016), a projection also seen in the high altitude regions of Tasmania to the south (Grose et al. 2010). We examine the balance

of parameterised rainfall (i.e., sub-grid scale estimates of rainfall, largely representing convective rainfall) and other precipitation types on the total rainfall projection, as well as projected changes to wet spells, dry spells and rainfall extremes, and examine the consistency of these projections to previous studies of rainfall processes.

2 Models and methods

Here we examine the projected changes in seasonal rainfall over mountain ranges, in all four calendar seasons (denoted by the initials of the months examined, i.e., DJF, MAM, JJA, SON) looking particularly at the peak seasons of JJA and DJF. We examine projected change in three RCM ensembles (Table 1), looking first at various mountain ranges in simulations performed for the Australian state of Queensland (https://app.longpaddock.qld.gov.au/climateFacts/) using the Cubic Conformal Atmospheric Model (CCAM) of McGregor and Dix (2008) at a global spatial resolution of ~ 50 km using the setup and methodology described by Katzfey et al. (2016), as used in Syktus and McAlpine (2016) and Salazar et al. (2016). At this ~ 50 km resolution, convection is fully parameterised. This ensemble is referred to as CCAM-50 for simplicity.

We then examine the Australian Alps in detail. Firstly, mean rainfall in 1990–2009 (the baseline used in model outputs), and linear trends in rainfall in 1970–2017 are examined using the Australian Gridded Climate Dataset (AGCD), which is a 0.05 °lat/lon (~ 5 km) gridded climate dataset based on observations (Jones et al. 2009). The mean circulation over regions is indicated by the mean wind speed at the 850 hPa level in NCEP/NCAR Reanalysis 1 (Kalnay et al. 1996), displayed as vectors. Precipitation projections for the Australian Alps in CCAM-50 and also two fine resolution RCM ensembles are examined. The first fine resolution ensemble is the new projections for the Australian state of Victoria using CCAM at ~ 5 km spatial resolution using the approach described by McGregor et al. (2016), which includes the downscaling digital filter of Thatcher and McGregor (2011), referred to as CCAM-5. The CCAM parameterisation for convection is scale-aware, so becomes increasingly weaker as the model approaches convective scales, hence in these ~ 5 km resolution simulations, the influence of the convective parameterisations is relatively weak. The second is the New South Wales and Australian

Table 1 Dynamical downscaling models and details used in this study

Ensemble name	Model	Resolution and domain	Input models	Emissions scenario and periods used
WRF-10 New South Wales and Australian Capital Territory regional climate modelling (NARCLIM) project (Evans et al. 2014)	Weather Research and Forecasting (WRF)	10 km, southeast Australia	4 CMIP3 Global Climate Models 1. CCCMA CGCM3.1-t47 (run 4) 2. CSIRO-Mk3.0 (run 1) 3. MPI-OM-ECHAM5 (run 1) 4. MIROC3.2-medres (run 1) Three different WRF configurations (12 total simulations)	SRES A2 Time-slices 1990–2009, 2020–2039 and 2060–2079
CCAM-50 Department of Science, Information, Technology, and Innovation (DSITI), Queensland state government (for methods see: Katzfey et al. 2016)	Conformal Cubic Atmospheric Model (CCAM)	50 km, global	11 CMIP5 GCMs (all run 1) 1. ACCESS-1.0 2. ACCESS-1.3 3. CCSM4 4. CNRM-CM5 5. CSIRO-Mk3.6 6. GFDL-CM3 7. GFDL-ESM2M 8. HadGEM2-CC 9. MIROC5 10. MPI-ESM-LR 11. NorESM1-M	RCP8.5 Continuous 1961–2100
CCAM-5 Victorian projections for Department of Environment, Land, Water and Planning (DELWP) and Wine Australia (for methods see: McGregor et al. 2016)	CCAM	5 km, southeast Australia	6 CMIP5 GCMs (all run 1) 1. ACCESS-1.0 2. CNRM-CM5 3. GFDL-ESM2M 4. HadGEM2-CC 5. MIROC5 6. NorESM1-M	RCP8.5 Continuous 1961–2100

Capital Territory Regional Climate Modelling project (NARCliM), which uses the Weather Research and Forecasting (WRF) model at ~ 10 km spatial resolution (Evans et al. 2014; Olson et al. 2016), referred to as WRF-10. All model ensembles reproduce the rainfall climatology of Australia with more fidelity than GCMs, including the higher rainfall over mountains, see listed publications for details of the evaluation, and see Figure S1 for an evaluation of CCAM-5 mean seasonal rainfall over the Australian Alps compared to AGCD and also high-resolution atmospheric Bureau of Meteorology Atmospheric high-resolution Regional Reanalysis for Australia (BARRA) at ~ 12 km resolution (Su et al. 2018).

Projected change is examined over a consistent timeframe of 1990–2009 to 2060–2079 under a high emissions scenario. The specific emissions pathway differ between the ensembles: both CCAM ensembles use the global climate models from the Coupled Model Inter-comparison Project phase 5 (CMIP5) ensemble as input (Taylor et al. 2012), which are forced by the representative concentration pathway (RCP) RCP8.5 (van Vuuren et al. 2011), whereas WRF-10 uses models from the CMIP3 archive (Meehl et al. 2007) and so uses climate forcings from the A2 emissions scenario from the special report on emissions scenarios (SRES) of Nakicenovic et al. (2000). The A2 scenario and RCP8.5 both feature ongoing high emission of greenhouse gases, however A2 has slightly lower concentrations than RCP8.5 by 2100. Forcings under each scenario are applied and dynamically modelled in each host GCM, but how the emissions scenarios are applied in RCMs makes a difference to the results (Jerez et al. 2018). Here the atmospheric forcings are also applied consistently in the relevant components of RCMs (e.g., radiation balance in each model). GCM data were interpolated to a common 2×2 °lat/lon grid, and all observed and RCM outputs were analysed using the original grids.

The projected change in (1) total rainfall; (2) sub-grid scale parameterised rainfall (largely representing convective rainfall, so is labelled 'convective'); and (3) the difference between 1 and 2, mainly representing large-scale and stratiform rainfall so is labelled 'stratiform' (but it should be noted that this also represents snow and graupel) are examined in all four calendar seasons (denoted by the initials of the months examined, i.e., DJF, MAM, JJA, SON). The projected change in the Expert Team on Climate Change Detection and Indices (ETCCDI) set of indices related to rainfall extremes and wet/dry periods (Karl et al. 1999) is examined in CCAM-50.

The configuration of the model in aspects such as convection or microphysics are likely to affect the projections, especially for convective rainfall change. WRF-10 uses three different configurations of WRF (Table 2). Configurations R1 and R3 use the Kain–Fritsch convection scheme (Kain 2004), whereas configuration R2 uses the Betts–Miller–Janjic scheme. The configuration R2 uses a cumulus physics scheme that was previously found to produce less rain (Gilliland et al. 2007). The CCAM convection scheme (McGregor 2003) handles both deep and shallow convection in a unified manner and employs a unique closure. The scheme calculates updraft mass fluxes, as used in the Kain–Fritsch scheme but not the Betts–Miller–Janjic. In this way, the CCAM scheme shares more similarities with the R1 and R3 configurations in WRF-10, than the R2 configuration.

Cases where the projected change in rainfall is enhanced on or near mountain ranges compared to surrounding regions are identified, and where there is a relationship between rainfall change and elevation are identified. For summer rainfall, regions where change in convective rainfall determines the direction of total rainfall change are also identified. Note here that the convective rainfall in the respective models is produced by a model parameterisation scheme and not modelled on first principles, so is sensitive to both the parameterisation used and the resolution of the model itself.

Table 2 Configuration of the 3 WRF regional climate models in WRF-10

Ensemble member	Planetary boundary layer physics/surface layer physics	Cumulus physics	Micro-physics	Land surface physics	Shortwave/long-wave radiation physics
R1	MYJ/Eta similarity	KF	WDM 5 class	Noah LSM	Dudhia/RRTM
R2	MYJ/Eta similarity	BMJ	WDM 5 class	Noah LSM	Dudhia/RRTM
R3	YSU/MM5 similarity	KF	WDM 5 class	Noah LSM	CAM/CAM

The planetary boundary layer physics/surface layer physics include Yonsei University (YSU)/Similarity theory (MM5) and Mellor–Yamada–Janjic (MYJ)/Similarity theory (Eta). The cumulus physics are Kain–Fritsch (KF) and Betts–Miller–Janjic (BMJ) schemes. The radiation physics include Dudhia/RRTM and CAM/CAM shortwave/long wave schemes. Other physics include microphysics (WDM 5 class) and land surface physics (Noah LSM)

3 Results

3.1 Mean rainfall in mid-latitude mountain ranges

We first look at the projected rainfall change over various mountain ranges in the mid-latitude belt of westerly circulation (25–50 °latitude) in the global medium-resolution RCM ensemble CCAM-50. This ensemble projects an enhanced rainfall decrease in winter (DJF in the northern hemisphere, JJA in the southern hemisphere) on or near four example mountain ranges (Fig. 1). The rainfall decrease appears enhanced as a proportional change on the windward slopes or near various European ranges including the western slopes of the European Alps, some regions within the Rocky Mountains in North America, the northern extent of the Andes in South America and southwest South Africa (Fig. 1). Here the 1000 m contour is shown as a guide to the location of major topography, and just four examples are shown. The results are broadly consistent with simulations of idealised mountain ranges (Shi and Durran 2014), where the decrease is proportionally greater at some regions of the windward slopes and higher altitude in the band of 40–50 °S. In addition, some mountain ranges in the 25–40 °S band in all sub-domains show a similar rainfall decrease on the windward slopes. The projected rainfall increase south of 50 °S in southern Chile is consistent with previous projections and idealised model simulations. The projections in the realistic mountain ranges are noisier and less clear compared to idealised mountains, but there are several cases that appear interesting.

Next we turn to summer rainfall change, where convective rainfall is a higher proportion of the total rainfall in mid-latitude mountains, and convective rainfall was previously found to be important to the total rainfall change (Giorgi et al. 2016). Projected changes in CCAM-50 for the European Alps in summer (Fig. 2a–d) broadly reproduce the results of Fischer et al. (2015) and Giorgi et al. (2016) despite the coarser resolution (~ 50 km compared to ~ 12 km). Namely, there is a projected rainfall increase at high altitude in contrast to the rainfall decrease in the broader region, where this sign of change is driven by a marked increase in convective rainfall and a smaller reduction in stratiform rainfall types above ~ 1000 m modelled altitude. In CCAM-50, convective rainfall is projected to increase more than an opposing decrease in stratiform rainfall in many regions around the world, not just on or near mountains (Fig. 2e, f). In the northern hemisphere summer (JJA), this balance is present at the top of European Alps as expected, but also in regions within other mountain ranges in Europe, Asia, North America and Africa and non-mountain regions in all continents. In the southern hemisphere summer (DJF), the same balance is present on the inland slopes of Australian Alps as expected from the high-resolution ensembles, but also present in many other regions including areas not near mountains.

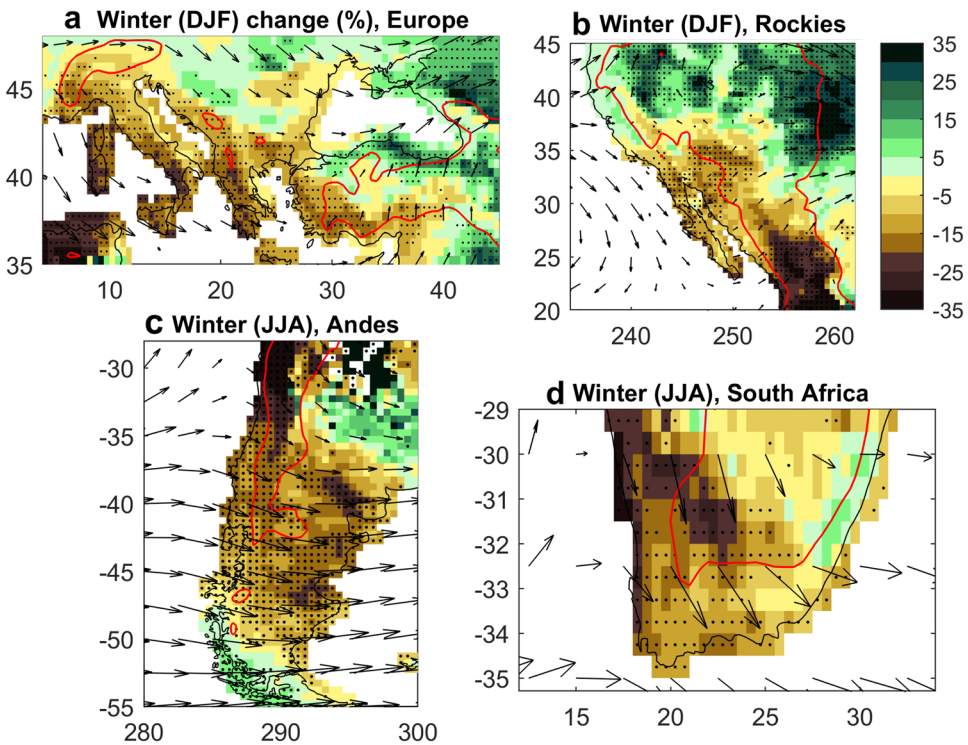

Fig. 1 Projected change in winter rainfall (%) in 11-member CCAM-50 ensemble between 1990–2009 and 2060–2079 under RCP8.5 in winter (DJF in northern hemisphere, JJA in southern hemisphere) in four regions as marked. Arrows indicate the mean 850 hPa winds in NCEP/NCAR Reanalysis 1 in 1990–2009 at 2.5°lat/lon spacing; stippling indicates where more than 8 out of 11 models agree on the sign of change; red line signifies the model's 1000 m elevation contour to indicate major topographic features

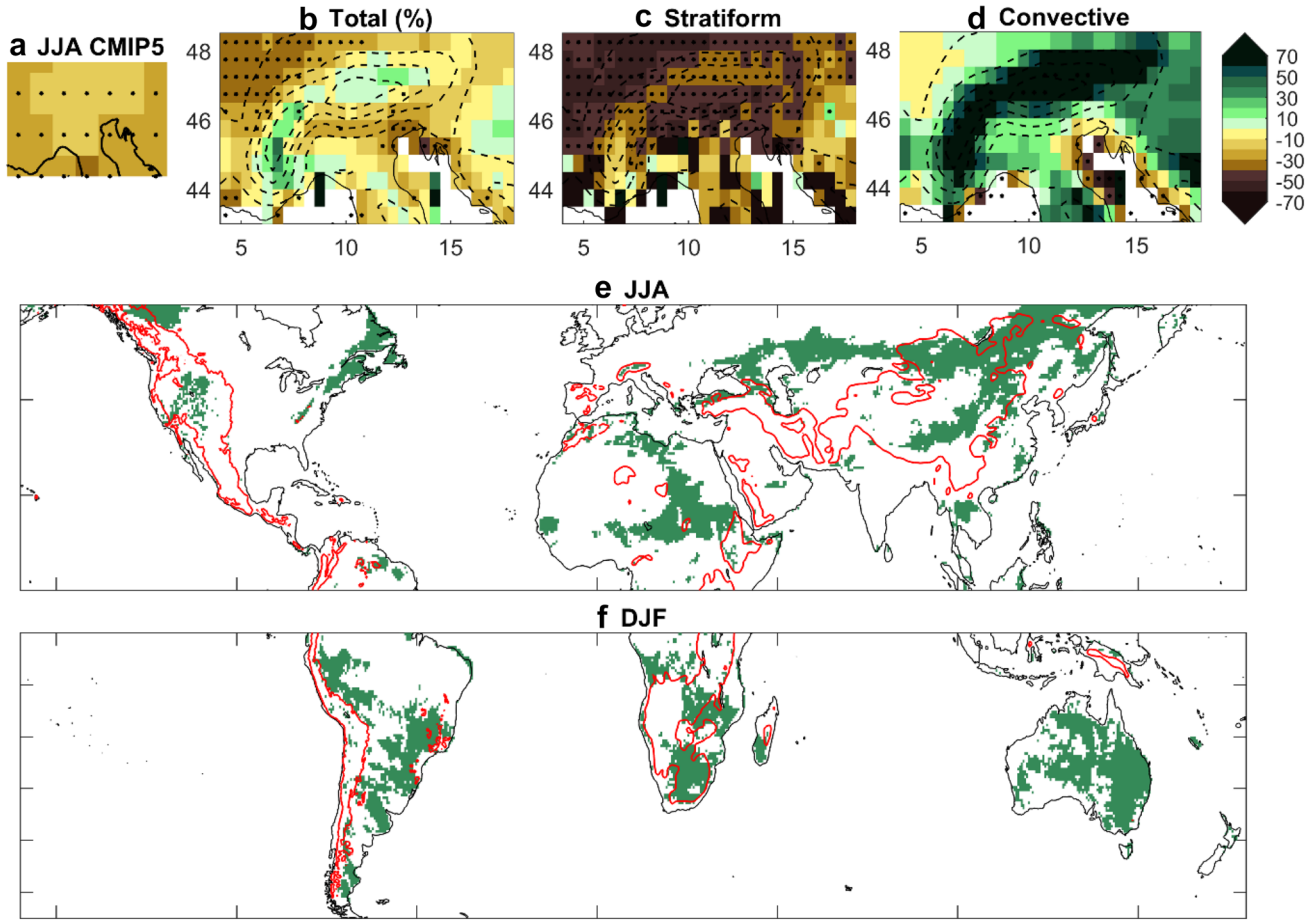

Fig. 2 Projected change in summer rainfall between 1990–2009 and 2060–2079 under RCP8.5 in the CCAM-50 ensemble mean, **a** the European Alps in 11 CMIP5 models; **b** Alps in CCAM-50 total rainfall; **c** Alps in CCAM-50 stratiform rainfall; **d** Alps in CCAM-50 convective rainfall; **e** areas where change in convective rainfall determines the sign of change in total rainfall in boreal summer (JJA); **f** as for **e** but for southern hemisphere summer (DJF). In the upper panels stippling indicates where 9–11 models agree on the sign of change and dashed lines indicate the model's surface height at 400 m intervals. In the lower panels, red lines show the 1000 m height contour to indicate major topographic features

3.2 Mean rainfall in the Australian Alps

We now turn to the Australian Alps as an example of lower elevation mountains in the mid-latitude westerly belt where we have two high-resolution RCM ensembles to compare to CCAM-50. In the Australian Alps, higher rainfall is seen over the mountains than over the lowlands with a distinct seasonal cycle peaking in winter, and a mean westerly circulation in all seasons (Fig. 3). There is high inter-annual variability in most seasons (see Fig. 3 caption, e.g., winter rainfall is 115 ± 36 mm/month).

Since 1970, the AGCD dataset shows the Australian Alps have seen an enhanced drying at higher altitude compared to the surrounding regions in autumn, winter and spring (with statistical significance of greater than $p = 0.1$ in some regions in autumn and spring), as found previously (Fiddes and Pezza 2015), as well as an increase in precipitation in summer in contrast to the rainfall decrease in surrounding areas (Fig. 3). More detailed analysis of rainfall trends in observations is not performed, as the AGCD dataset has poor station coverage over the Alps and so trend analysis can't be considered completely reliable. Further analysis using additional datasets or high-resolution reanalysis is needed.

Turning to model projections, in the cooler seasons outside summer (MAM, JJA, SON), there are various cases where the RCM project an enhanced rainfall decrease on the windward slopes or otherwise in the proximity of the Australian Alps (Figs. 4, 5, 6). The projection of enhanced rainfall decrease on windward slopes in the cool season is consistent with previous projections, other regions shown above and idealised simulations (e.g. Shi and Durran 2014).

In CCAM-5 there is an enhancement of the projected decrease in total rainfall on the inland, windward slopes in

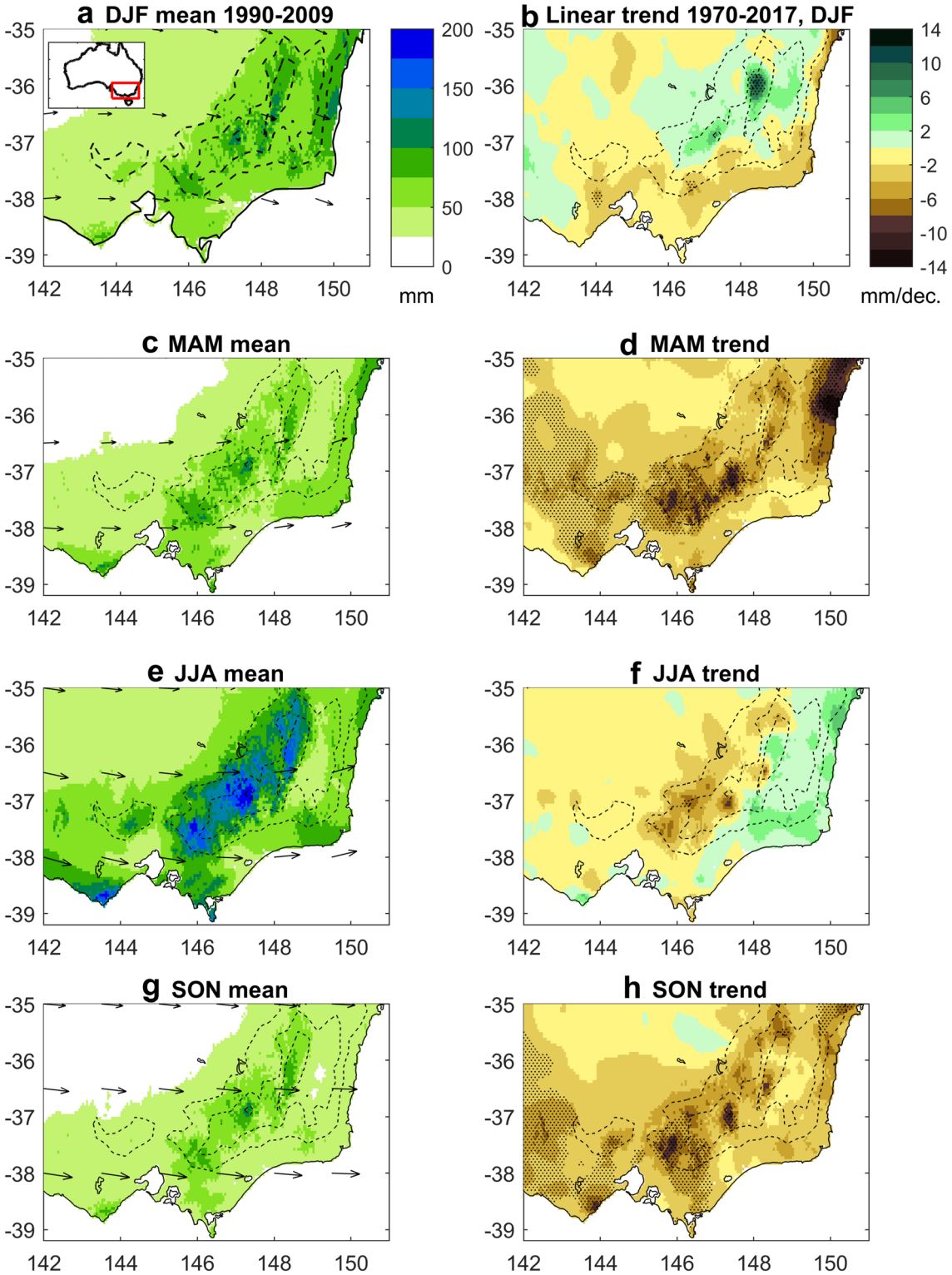

Fig. 3 Rainfall mean and trends in the AGCD dataset, **a** mean rainfall in 1990–2009 in Summer (DJF), rainfall > 1000 m elevation is 83 ± 30 mm/month (mean and standard deviation), inset shows the location of the Australian Alps domain within Australia, vectors show the mean 850 hPa wind; **b** linear trend in mean rainfall in 1970–2017 (mm/decade) in DJF; **c** mean in Autumn (MAM), rainfall > 1000 m elevation 83 ± 32 mm/month; **d** trend in MAM; **e** mean in winter (JJA), rainfall > 1000 m elevation is 115 ± 36 mm/month; **f** trend in JJA; **g** mean in spring (SON), rainfall > 1000 m elevation is 108 ± 32 mm/month; **h** trend in SON. Dashed lines show topography at contours of 400 m, hatching shows statistical significance of the linear trend at the 0.1 level

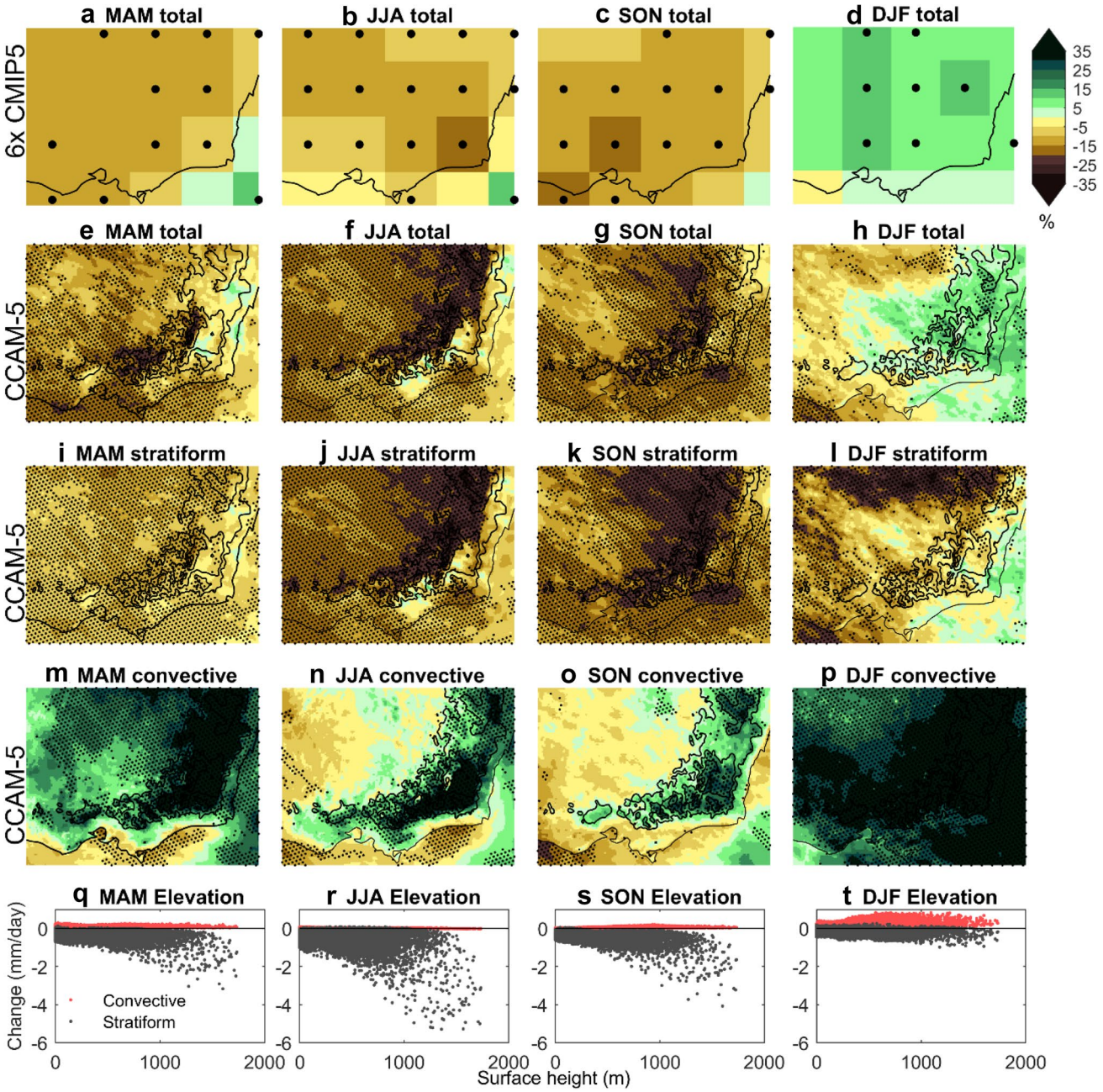

Fig. 4 Projected change in rainfall in the Australian Alps in CCAM-5 between 1990–2009 and 2060–2079 under RCP8.5 (%) by calendar season, **a** autumn (MAM); **b** winter (JJA) and **c** spring (SON). First row shows change in total rainfall in the mean of 6 CMIP5 models used as input; second row shows CCAM-5 total rainfall; third row is CCAM-5 stratiform rainfall; fourth row is CCAM-5 convective rainfall; and fifth row plots modelled surface height against convective and stratiform rainfall change. Stippling indicates where 5 or 6 models agree on the sign of change, lines show coastline and model topography contours at 400 m intervals

MAM, JJA and SON seasons (Fig. 4e–g) compared to the six CMIP5 models used as input (Fig. 4a–c). The decreases in stratiform rainfall types (Fig. 4i–k) exceeded a slight increase in convective rainfall over the mountains. While the change in convective rainfall is large as a proportion (%), convective rainfall is very low in these seasons so represents a small change in absolute rainfall (discernible in scatter plots, Fig. 4q–s). The rainfall decline in stratiform rainfall appears to have some elevation-dependence in autumn, winter and particularly in spring, but the only relationship that is significant at the 95% level in stratiform rainfall in spring (using the t-statistic of the linear coefficient).

The WRF-10 ensemble shows some similar projected changes as CCAM-5 in the cool seasons, but some notable

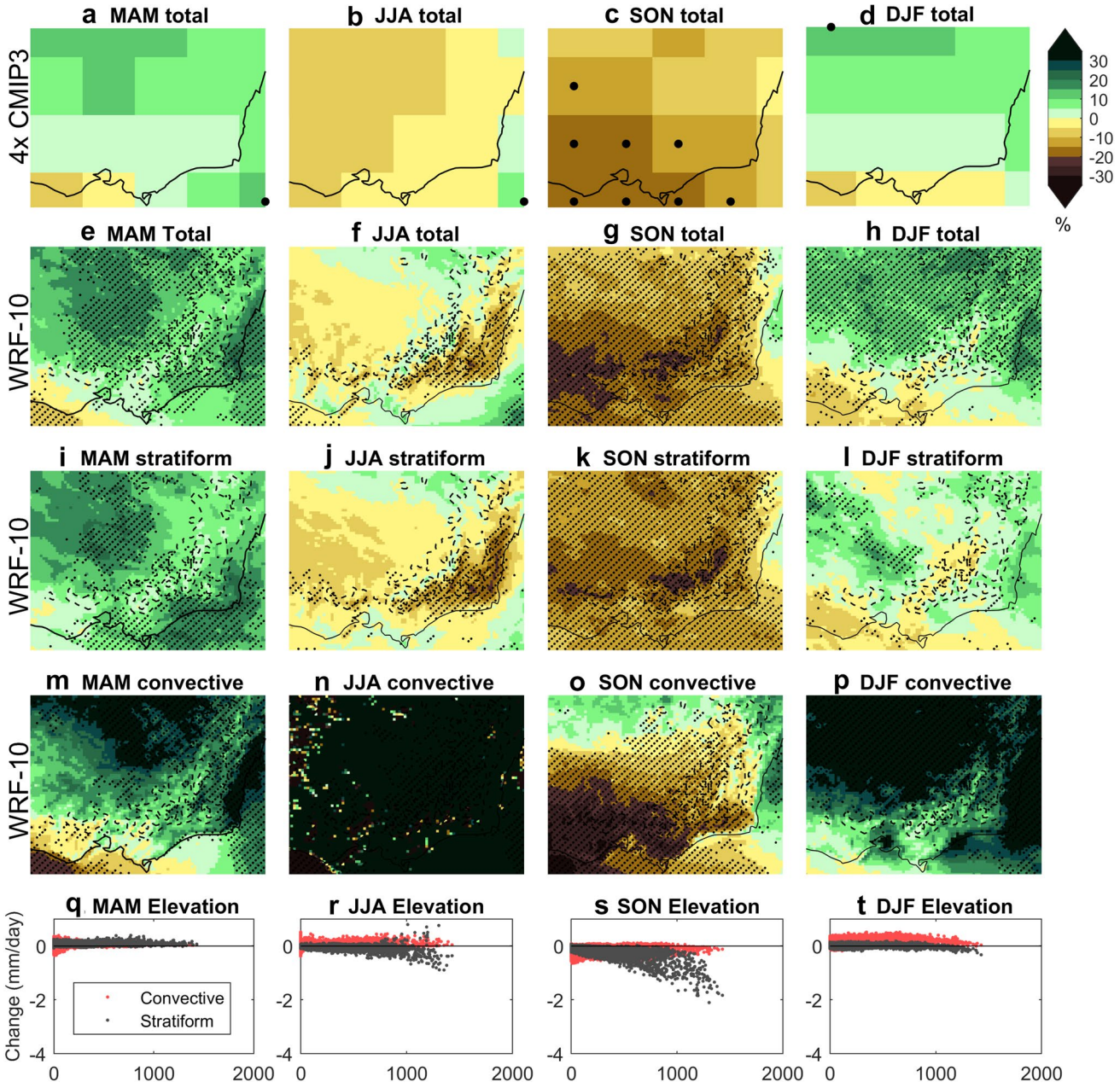

Fig. 5 As for Fig. 4 but for the WRF-10 ensemble and under the A2 scenario, stippling indicates where 9–12 simulations agree on the sign of change

differences in the seasonal signature (Fig. 5). Winter rainfall is projected to decrease but not as strongly as in CCAM-5, whereas the strong spring rainfall decline is similar to CCAM-5. The autumn rainfall projection is wetter than CCAM-5, driven by a difference in the GCMs used as input and expressed through the change in stratiform rainfall (WRF-10 projections of convective rainfall is similar to CCAM-5). There appears to be elevation dependence in some cases such as spring, but no slope is significant at 95% in WRF-10 in any season. In some cases in both WRF-10 and CCAM-5, the relationship to topography appears to be complex (e.g. stronger on one slope than the other), so a simple linear fit of change and elevation doesn't capture the relationship.

The lower resolution CCAM-50 shows a similar projection as CCAM-5, but with lower magnitude of drying and less fine-scale spatial detail around the peaks (Fig. 6). This suggests that the added value in the change signal of enhanced drying over mountains is present even with coarsely resolved mountains, but the magnitude of projected

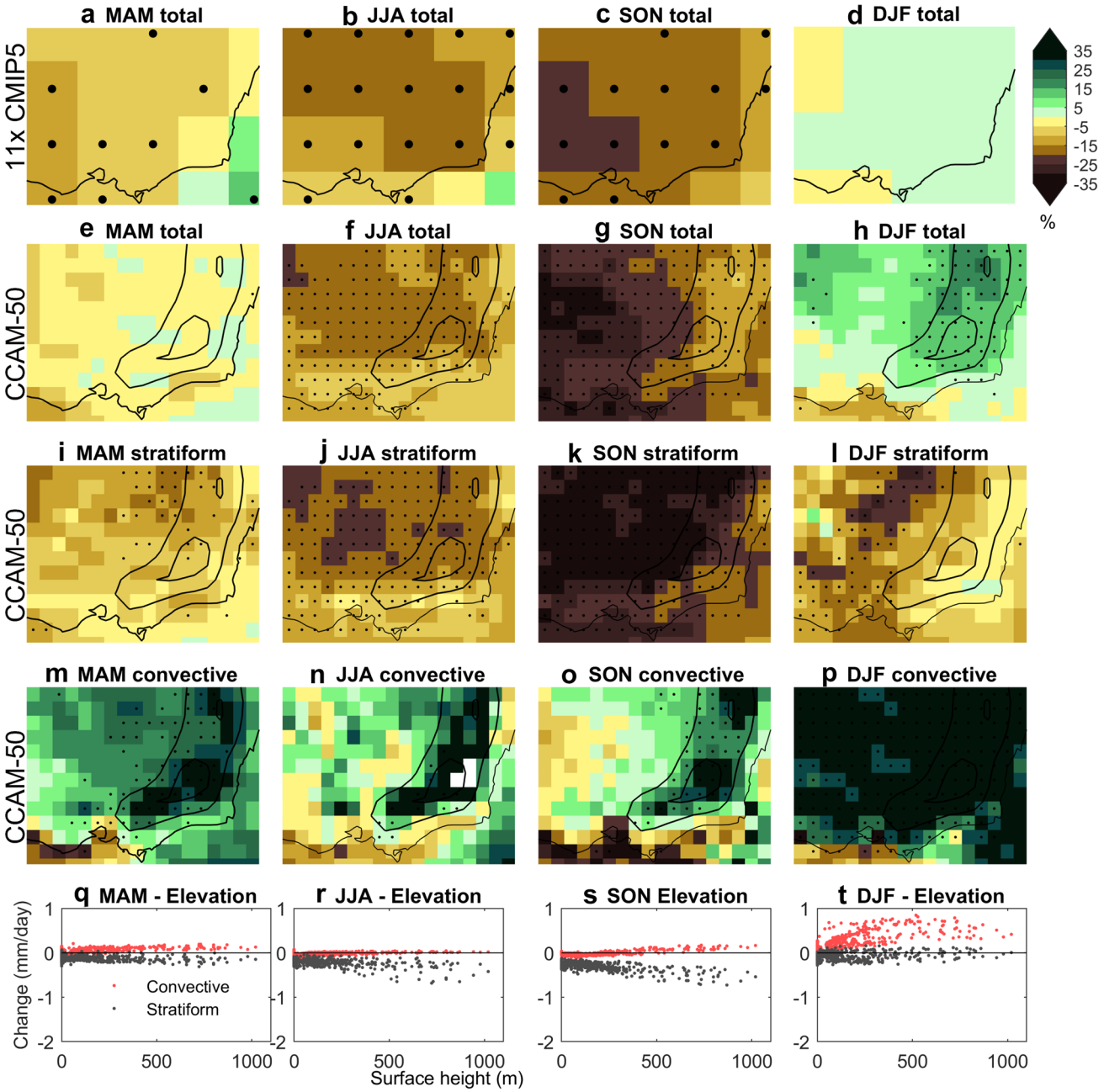

Fig. 6 As for Fig. 4 but for the CCAM-50 ensemble, stippling indicates where 9–11 simulations agree on the sign of change, dashed lines show model topography contours at 400 m intervals

change increases with the resolution of the topography features.

In summer, there is some similarity in the projected change between all three high-resolution ensembles, with some degree of enhanced rainfall increase on or near the Australian Alps (Figs. 4, 5, 6). In CCAM-5 in summer (Fig. 4), convective rainfall shows an increase with elevation-dependence (positive slope is significant at the 95% confidence level), and this change determines the sign of change in total rainfall in much of the region. The same balance of projected changes was seen in the coastal slopes in CCAM-5 in MAM rainfall. In WRF-10, the projection of convective and stratiform rainfall is similar to CCAM-5, but with less obvious elevation-dependence in convective rainfall change (Fig. 5). The results from CCAM-50 are similar to CCAM-5 despite the lower resolution (Fig. 6), suggesting that the model configuration has a greater effect

on the projections than the resolution within this range (between 5 and 50 km).

Looking at rainfall averaged over the highlands region (above 1000 m modelled altitude), there is a projected reduction in the seasonal cycle expected from the seasonal means above, but with a wide model range and some difference between CCAM-5 and WRF-10 (Fig. 7). CCAM-50 is not examined, as it doesn't resolve peaks over 1000 m. There is generally a reduction in the cool season total rainfall but a different seasonal signature in the two ensembles, e.g., a reduction in CCAM-5 but little change in WRF-10 in autumn (Fig. 7). In summer there is little change or a small increase in total rainfall with lower model agreement in both CCAM-5 and WRF-10. Convective rainfall is projected to increase in summer, with higher model agreement in CCAM-5 than WRF-10 (Fig. 7c, d).

The wider range of results in WRF-10 is due in part to the marked differences between the three different WRF configurations used compared to a single setup in CCAM. The convection or microphysics schemes in the three WRF configurations (Table 2) give a different mean in the current climate and in the projected change. In particular, configuration R2 simulates lower convective rainfall in some regions in summer (Fig. 7), and also a lower projected change in convective rainfall in summer (Fig. 8). The lower consistency in the projections from WRF-10 compared to CCAM-5 in all seasons is also likely a function of the limited-area model with uncorrected GCM inputs used in WRF-10 compared to

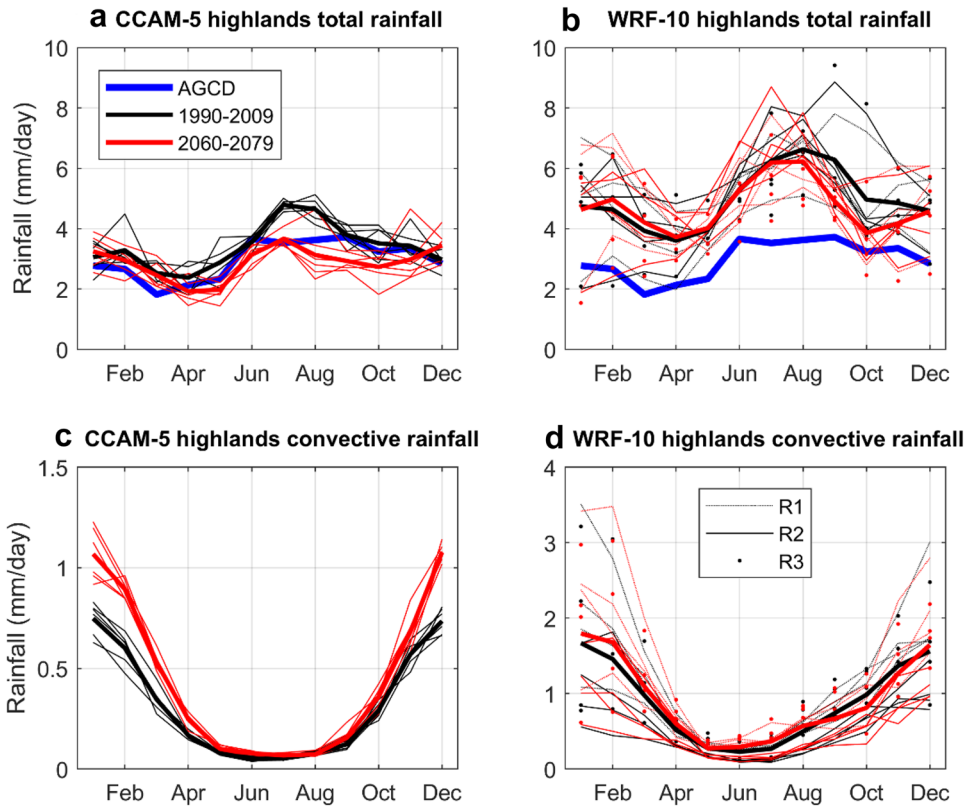

Fig. 7 Monthly mean rainfall above 1000 m modelled altitude in the Australian Alps in each month of the year in AGCD observed dataset in 1990–2009 (blue), modelled in 1990–2009 (black) and modelled in 2060–2079 (red) in each simulation (thin lines) and the mean of simulations (thick lines) for: **a** total rainfall in six CCAM-5 simulations; **b** total rainfall in twelve WRF-10 simulations; **c** convective rainfall in CCAM-5; **d** convective rainfall in WRF-10, line styles in WRF-10 plots represent the three different model configurations used (R1, R2 and R3)

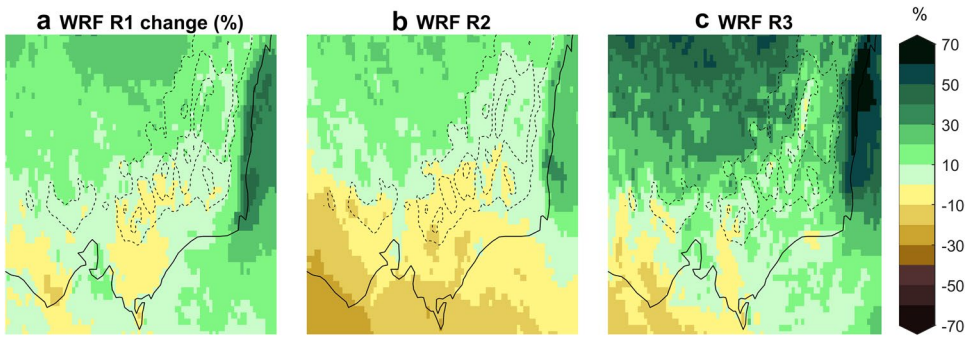

Fig. 8 Projected change in DJF convective rainfall (%) in the three configurations of WRF used in WRF-10 (four simulations per sample)

the global atmospheric model that uses only corrected sea surface temperatures (SSTs) and sea ice from GCMs used in CCAM (Thatcher and McGregor 2011). Both WRF-10 and CCAM-5 chose their subset GCM host models to be representative of the range of change in the respective ensembles (CMIP3 and CMIP5), however the GCM choice seems to explain some difference in the projections for Autumn (MAM).

3.3 ETCCDI indices

Looking at winter as indicative of the cool seasons, and examining both the European and Australian Alps, there are some notable features in the projections of ETCCDI indices. CCAM-50 shows an influence from topography in the projected changes in wet days, consecutive wet days, wet day precipitation and maximum 5-day rainfall (Fig. 9). Similar changes are also seen in heavy precipitation days, very heavy precipitation days, consecutive dry days, simple daily intensity, very wet day precipitation, extreme wet day precipitation and maximum 1-day precipitation (European case shown in Figure S2). See Karl et al. (1999) for the general definitions of ETCCDI indices, and Wong et al. (2011) for the derivation of theses indices for the CCAM-50 ensemble. The results for the Australian Alps from CCAM-50 are similar to that previously found in WRF-10 for the same indices such as maximum 1-day precipitation (Evans et al. 2016). In contrast to winter, there is an enhanced projected

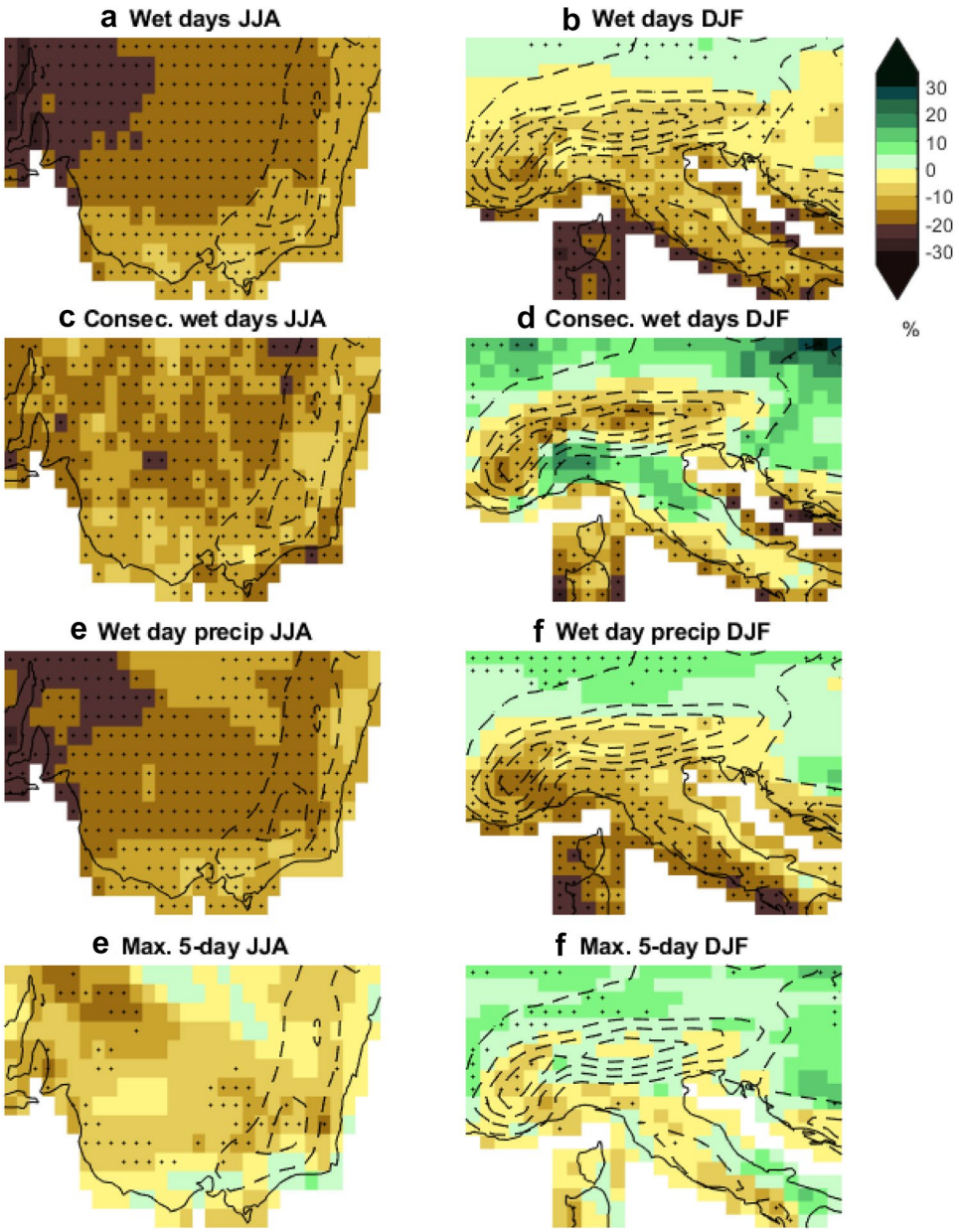

Fig. 9 Projected change in expert team on climate change detection and indices (ETCCDI) rainfall indices in CCAM-50 for 1990–2009 to 2060–2079 under RCP8.5 in winter for the Australian Alps and European Alps, mean of 11 ensemble members, stippling indicates where 9–11 simulations agree on the sign of change. Dashed lines show modelled topography contours at 400 m intervals: **a, b** count of wet days over 1 mm; **c, d** maximum number of consecutive wet days over 1 mm; **e, f** precipitation on wet days (mm/day); maximum precipitation of consecutive 5-day periods (mm)

increase in ETCCDI indices in summer (Figure S3), as found by Fischer et al. (2015).

4 Discussion

Here the projected changes in precipitation over mid-latitude mountain ranges between the start and late twenty-first Century under a high emissions scenario is examined in intermediate (~ 50 km) and high resolution (~ 5 and ~ 10 km) RCM ensembles. Projected changes in all three ensembles show notable differences from the coarser models used as input, including small-scale spatial detail associated with topography. This is conceptually known as 'downscaling signal' (Di Luca et al. 2012), as documented previously in WRF-10 by Di Luca et al. (2016).

Projected rainfall changes in cooler seasons appear to be consistent with simulations using idealised mountain ranges, with enhanced drying over the windward side of mountain ranges driven by changes in stratiform (non-convective) rainfall rather than convective rainfall. This projection is suggested for high mountain ranges such as the western slopes of the European Alps, but is present in the much lower Australian Alps where there is a greater projected decrease in rainfall on the windward slopes or otherwise in the proximity of the Australian Alps compared to the lower altitude in winter and spring in all three RCM ensembles. This enhancement is found on the inland slopes and tops of mountains in some cases but is strongest on the windward slopes in some cases. An enhanced rainfall reduction in winter mean rainfall is also seen on windward slopes or tops of other mid-latitude mountain ranges, and a projected decrease in various rainfall extremes indices is seen in the Australian Alps and European Alps in winter.

Previous studies suggest that in mid-latitude mountains this enhanced decrease is driven by changes such as a decrease in saturated vertical displacement (Shi and Durran 2014), shifts in the pattern of condensation with warming (Siler and Roe 2014), and possibly an increase in weak rain shadows (Siler and Durran 2016). The results presented here are broadly consistent with these previous results, and are quite consistent among the ensembles with different resolutions and configurations, and in realistic mountains rather than idealised mountain ranges. This suggests that the physical mechanisms such as decreases in saturated vertical displacement can be expected to drive rainfall decreases in mid-latitude mountain ranges in the future. A switch from precipitation as snow to rain may also contribute to particularly strong decreases on the upper slopes in winter, as found in idealised high-resolution experiments in the Rocky Mountains (Pavelsky et al. 2012). This is less likely to be an important driver in mountains with small and marginal snow cover such as the Australian Alps. Also, large-scale processes driving increases in wet extremes are in fact less sensitive over mountains (Shi and Durran 2016), suggesting a decrease in wet extremes over mountains compared to lower elevation, and this is consistent with projections over the European Alps in winter presented here (Figure S2).

Projected rainfall change in mid-latitude mountains in summer is more dependent on changes in smaller-scale processes such as convection than the cool season, since convective rainfall is a larger component of the total rainfall. The projected change to convective rainfall determines the sign of total change of rainfall on the inland slopes of the Australian Alps, and near some other mid-latitude mountains, but also in other regions away from mountain ranges. The response over mountains is consistent with RCM rainfall projections in European Alps (Giorgi et al. 2016), and with enhancement of convective rainfall with warming at this latitude (Cannon et al. 2012). Enhanced increases in wet extremes over the mountains in summer is consistent with previous studies (Fischer et al. 2015), and is likely to be driven by convective processes such as convection consistent with extremes in this season (Shi and Durran 2015). However, the response in non-mountain regions may involve other processes, and needs further examination.

For the Australian Alps, projections show some notable similarity to recent trends, namely an enhanced drying over the higher elevations in the cool seasons but a rainfall increase in contrast to surrounding drying in summer (Fig. 3). Biases or other limitations of the observed datasets should be noted. The observed trends suggest that an effect of greenhouse gases on rainfall trends may be already present and attributable in the current climate, but this also requires further work.

Next we consider how the model choices of resolution, emissions scenario and convection scheme affect the results. In the cool seasons, the magnitude of the projected rainfall reduction and enhancement around the Australian Alps is lower in CCAM-50 compared to CCAM-5 in some notable cases. This indicates that the resolution of the topography and the meso-scale features in simulations implies an enhancement of rainfall reductions over mountains in all cases, but the resolution affects the magnitude of rainfall change over the peaks in cool seasons.

In summer, projected changes in the total, convective and stratiform precipitation types for the Australian Alps from the intermediate resolution CCAM-50 ensemble (~ 50 km, with fully parameterised convection) are broadly similar to the fine resolution CCAM-5 ensemble (~ 5 km, where convection is modelled to a greater extent and parameterisations are weak). CCAM-50 also reproduces similar results for the European Alps published previously. This similarity of results suggests that the effect of the CCAM convection parameterisations is similar to the modelled convection down to this resolution. It would

be informative to look at simulations at 'convection-permitting' resolution of (~ 1.5 km) is used (e.g. Kendon et al. 2017). As expected, the different configurations of convection or microphysics in the three WRF model configurations used in WRF-10 give different projected changes (Fig. 8). This is consistent with previous analysis of WRF ensembles (Evans et al. 2012; Katragkou et al. 2015). In particular, the configuration R2, which includes the Betts–Miller–Janjic convection scheme, produces lower convective rainfall and a weaker convective rainfall response than R1 and R3, consistent with previous results in Gilliland et al. (2007). The CCAM convection scheme shares more similarities with the R1 and R3 configurations than the R2 configuration, consistent with a stronger response in convective rainfall in all these ensembles. Previous studies also suggest the convection scheme has an effect on the projections, where a set of recent RCMs projected a rainfall increase on the European Alps in summer (Fischer et al. 2015), but drying extended to the tops of the Alps in an earlier set of RCMs (Gobiet et al. 2014), perhaps due to the handling of convection. The convection scheme has been found to affect the simulation of phenomena that bring heavy rainfall, including the intensity of extra-tropical cyclones (Ragone et al. 2018). The effect of different convection schemes on the projected changes in rainfall and the weather systems that bring them requires further investigation, where if particular convection schemes can be shown to be more or less appropriate then this could provide a more reliable projections of change, including in cases such as the European Alps.

In CCAM-50 the influence of convective rainfall change in determining the direction of summer total rainfall change seems to be only loosely proportional to the strength of forcing from greenhouse gases. In the European Alps, the projected increase on mountains was clear in projections under the strong forcing of RCP8.5 through different periods in the century in Giorgi et al. (2016), and was present in the multi-model ensemble under lower forcing of A1B in Fischer et al. (2015). Here, the cases where convective rainfall change determines the sign of change in total rainfall in summer, for the 1990–2009 to 2060–2079 case, are fairly consistent in 1990–2009 to 2020–2039 change (Figure S4).

The results hold implications for interpreting the output from analogue-based statistical downscaling for projected change in summer rainfall. If the method used does not account for changes in processes such as convection, then it may not project the sign of change in summer rainfall reliably. In fact, it was previously found that statistical downscaling can give opposite sign of projected rainfall change under a warming climate depending on the predictors used (Fu et al. 2018).

5 Conclusion

The results suggest an enhancement of the drying on the slopes or tops of mid-latitude mountain ranges in the cool season, including in the Australian Alps, is plausible due to increasing greenhouse gases and a warmer climate. The projections in broadly consistent with changes found in idealised experiments (Shi and Durran 2014), so is consistent with large-scale circulation changes together with changes in drivers such as saturated vertical displacement. A projected increase in summer rainfall near the peaks of the Australian Alps is driven in part by an increase in convective rainfall, which shows some similarity to the case in the European Alps (Giorgi et al. 2016). Results from an ensemble of 50-km simulations suggest that change in convective rainfall may be important in determining the sign of summer rainfall change in a notable proportion of land regions, not exclusively in the vicinity of mountains. The results also suggest that it is useful to break down projections of different rainfall types (convective and stratiform) in the summer season and examine simplified models of underlying processes to examine the overall projected change in summer rainfall and assess confidence in projected changes.

The results show a potential usefulness of RCMs, revealing that the projected change in the mean seasonality of rainfall over mid-latitude mountain ranges such as the Australian Alps could be more strongly affected by human induced climate change than GCMs suggest. In particular, RCMs project a greater decrease at high altitude in cool seasons than GCMs and little change or rainfall increase in summer effectively reducing the seasonal cycle. This projected change would have flow-on effects to water management, stream flows, hydro-electric power generation, natural ecosystems and agriculture in the mountain regions, as well as downstream impacts on catchments originating in the mountains. This finding holds many implications for water management over or near other mountain regions, as well as many regions in summer (not just over mountains).

The results reinforce the value of supplementing lower resolution GCMs for examining projected climate change in regions with important surface forcing from topography. This further analysis may be in the form of additional statistical analysis specifically designed for rainfall over topography (e.g. Paeth et al. 2017), or higher resolution modelling as used here. For summer in particular, there may be value in examining convection-permitting resolution modelling (e.g. Ban et al. 2015; Prein et al. 2015; Kendon et al. 2017) to better assess projected rainfall over mountains.

Acknowledgements This work was supported by the Australian Government's National Environmental Science Program's Earth System and Climate Change hub, the Victorian Government's Department of Environment Land Water and Planning climate projections 2019

project (VCP19), Queensland Climate Adaptation Strategy (Q-CAS) and the Wine Australia Institute climate project. We thank John McGregor and Jack Katzfey from CSIRO for additional modelling support, helpful advice and assistance.

References

Ban N, Schmidli J, Schär C (2015) Heavy precipitation in a changing climate: does short-term summer precipitation increase faster? Geophys Res Lett 42:1165–1172

Beniston M, Stoffel M (2014) Assessing the impacts of climatic change on mountain water resources. Sci Total Environ 493:1129–1137

Cannon DJ, Kirshbaum DJ, Gray SL (2012) Under what conditions does embedded convection enhance orographic precipitation? Q J R Meteorol Soc 138:391–406

Chou C, Chen C-A, Tan P-H, Chen KT (2012) Mechanisms for global warming impacts on precipitation frequency and intensity. J Clim 25:3291–3306

Collins M et al (2013) Long-term climate change: projections, commitments and irreversibility. In: Stocker TF, Qin D, Plattner G-K et al (eds) Climate change 2013: the physical science basis. Contribution of working group I to the fifth assessment report of the intergovernmental panel on climate change. Cambridge University Press, Cambridge, pp 1029–1136. https://doi.org/10.1017/CBO9781107415324.024

Dezfuli AK, Zaitchik BF, Badr HS, Evans J, Peters-Lidard CD (2017) The role of low-level, terrain-induced jets in rainfall variability in tigris–euphrates headwaters. J Hydrometeorol 18:819–835

Di Luca A, Elía R, Laprise R (2012) Potential for small scale added value of RCM's downscaled climate change signal. Clim Dyn 40:601–618

Di Luca A, Argüeso D, Evans JP, de Elía R, Laprise R (2016) Quantifying the overall added value of dynamical downscaling and the contribution from different spatial scales. J Geophys Res Atmos 121:1575–1590

Eidhammer T, Grubišić V, Rasmussen R, Ikdea K (2018) Winter precipitation efficiency of mountain ranges in the colorado rockies under climate change. J Geophys Res Atmos. https://doi.org/10.1002/2017JD027995

Evans J, Ekström M, Ji F (2012) Evaluating the performance of a WRF physics ensemble over South-East Australia. Clim Dyn 39:1241–1258

Evans JP, Ji F, Lee C, Smith P, Argüeso D, Fita L (2014) Design of a regional climate modelling projection ensemble experiment; NARCliM. Geosci Model Dev 7:621–629

Evans JP, Argüeso D, Olson R, Di Luca A (2016) Bias-corrected regional climate projections of extreme rainfall in south-east Australia. Theor Appl Climatol. https://doi.org/10.1007/s00704-016-1949-9

Fiddes SL, Pezza AB (2015) Current and future climate variability associated with wintertime precipitation in alpine Australia. Clim Dyn 44:2571–2587

Fiddes SL, Pezza AB, Barras V (2015) Synoptic climatology of extreme precipitation in alpine Australia. Int J Climatol 35:172–188

Fischer AM, Keller DE, Liniger MA, Rajczak J, Schär C, Appenzeller C (2015) Projected changes in precipitation intensity and frequency in Switzerland: a multi-model perspective. Int J Climatol 35:3204–3219

Fu G, Charles SP, Chiew FHS, Ekström M, Potter NJ (2018) Uncertainties of statistical downscaling from predictor selection: equifinality and transferability. Atmos Res 203:130–140

Gao X, Xu Y, Zhao Z, Pal JS, Giorgi F (2006) On the role of resolution and topography in the simulation of East Asia precipitation. Theor Appl Climatol 86:173–185

Gilliland EK, Lincoln NE, Rowe CM (2007) A comparison of cumulus parameterization schemes in the WRF model. In: 87th American meteorological society meeting. San Antonio, Texas, USA

Giorgi F, Hurrell JW, Marinucci MR, Beniston M (1997) Elevation dependency of the surface climate change signal: a model study. J Clim 10:288–296

Giorgi F, Torma C, Coppola E, Ban N, Schar C, Somot S (2016) Enhanced summer convective rainfall at Alpine high elevations in response to climate warming. Nat Geosci 9:584–589

Gobiet A, Kotlarski S, Beniston M, Heinrich G, Rajczak J, Stoffel M (2014) 21st century climate change in the European Alps—a review. Sci Total Environ 493:1138–1151

Grose M, Barnes-Keoghan I, Corney S, White C, Holz G, Bennett J, Gaynor S, Bindoff N (2010) Climate futures for Tasmania: general climate impacts technical report. Hobart, Australia, Antarctic Climate and Ecoststems CRC

Harris RMB, Remenyi T, Bindoff NL (2016) The potential impacts of climate change on victorian alpine resorts. A Report to the Alpine Resorts Co-ordinating Council. Hobart, Australia, Antarctic Climate and Ecosystems Cooperative Research Centre

Held IM, Soden BJ (2006) Robust responses of the hydrological cycle to global warming. J Clim 19:5686–5699

Im ES, Coppola E, Giorgi F, Bi X (2010) Local effects of climate change over the Alpine region: a study with a high resolution regional climate model with a surrogate climate change scenario. Geophys Res Lett 37:6

Jerez S, López-Romero JM, Turco M, Jiménez-Guerrero P, Vautard R, Montávez JP (2018) Impact of evolving greenhouse gas forcing on the warming signal in regional climate model experiments. Nat Commun 9:1304

Jones DA, Wang W, Fawcett R (2009) High-quality spatial climate data-sets for Australia. Aust Meteorol Oceanogr J 58:233–248

Kain JS (2004) The Kain–Fritsch convective parameterization: an update. J Appl Meteorol 43:170–181

Kalnay E et al (1996) The NCEP/NCAR 40-year reanalysis project. Bull Am Meteorol Soc 77:437–471

Karl TR, Nicholls N, Ghazi A (1999) CLIVAR/GCOS/WMO Workshop on indices and indicators for climate extremes workshop summary. In: Karl TR, Nicholls N, Ghazi A (eds) Weather and climate extremes: changes, variations and a perspective from the insurance industry. Springer, Dordrecht, pp 3–7. https://doi.org/10.1007/978-94-015-9265-9_2

Katragkou E et al (2015) Regional climate hindcast simulations within EURO-CORDEX: evaluation of a WRF multi-physics ensemble. Geosci Model Dev 8:603–618

Katzfey JJ et al (2016) High-resolution simulations for Vietnam—methodology and evaluation of current climate. Asia Pac J Atmos Sci 52:91–106

Kendon EJ et al (2017) Do convection-permitting regional climate models improve projections of future precipitation change? Bull Am Meteorol Soc 98:79–93

Kotlarski S, Bosshard T, Lüthi D, Pall P, Schär C (2012) Elevation gradients of European climate change in the regional climate model COSMO-CLM. Clim Change 112:189–215

Leung LR, Ghan SJ (1999) Pacific northwest climate sensitivity simulated by a regional climate model driven by a GCM. Part II: 2 × CO_2 simulations. J Clim 12:2031–2053

McGregor JL (2003) A new convection scheme using a simple closure. BMRC Res Rep 93:33–36

McGregor JL, Dix MR (2008) An updated description of the conformal-cubic atmospheric model. In: Hamilton K, Ohfuchi W (eds) High resolution simulation of the atmosphere and ocean. Springer, New York, pp 51–76

McGregor JL, Nguyen KC, Kirono DGC, Katzfey JJ (2016) High-resolution climate projections for the islands of Lombok and

Sumbawa, Nusa Tenggara Barat Province, Indonesia: challenges and implications. Clim Risk Manag 12:32–44

Meehl GA, Covey C, Delworth T, Latif M, McAvaney B, Mitchell JFB, Stouffer RJ, Taylor KE (2007) The WCRP CMIP3 multimodel dataset—a new era in climate change research. Bull Am Meteorol Soc 88:1383–1394

Minder JR, Letcher TW, Liu C (2018) The character and causes of elevation-dependent warming in high-resolution simulations of rocky mountain climate change. J Clim 31:2093–2113

Nakicenovic N et al (2000) Special report on emissions scenarios. A special report of working group III of the intergovernmental panel on climate change. Cambridge University Press, Cambridge

Olson R, Evans JP, Di Luca A, Argüeso D (2016) The NARCliM project: model agreement and significance of climate projections. Clim Res 69:209–227

Paeth H, Pollinger F, Mächel H, Figura C, Wahl S, Ohlwein C, Hense A (2017) An efficient model approach for very high resolution orographic precipitation. Q J R Meteorol Soc 143:2221–2234

Pavelsky TM, Sobolowski S, Kapnick SB, Barnes JB (2012) Changes in orographic precipitation patterns caused by a shift from snow to rain. Geophys Res Lett. https://doi.org/10.1029/2012GL052741

Prein AF et al (2015) A review on regional convection-permitting climate modeling: demonstrations, prospects, and challenges. Rev Geophys 53:323–361

Ragone F, Mariotti M, Parodi A, Von Hardenberg J, Pasquero C (2018) A climatological study of western mediterranean medicanes in numerical simulations with explicit and parameterized convection. Atmosphere 9:397

Rangwala I, Miller JR (2012) Climate change in mountains: a review of elevation-dependent warming and its possible causes. Clim Change 114:527–547

Salazar A, Katzfey JJ, Thatcher M, Syktus JI, Wondg K, McAlpine C (2016) Deforestation changes land–atmosphere interactions across South American biomes. Glob Planet Change 139:97–108

Shi X, Durran DR (2014) The response of orographic precipitation over idealized midlatitude mountains due to global increases in CO_2. J Clim 27:3938–3956

Shi X, Durran DR (2015) Estimating the response of extreme precipitation over midlatitude mountains to global warming. J Clim 28:4246–4262

Shi X, Durran D (2016) Sensitivities of extreme precipitation to global warming are lower over mountains than over oceans and plains. J Clim 29:4779–4791

Siler N, Durran D (2016) What causes weak orographic rain shadows? Insights from case studies in the cascades and idealized simulations. J Atmos Sci 73:4077–4099

Siler N, Roe G (2014) How will orographic precipitation respond to surface warming? An idealized thermodynamic perspective. Geophys Res Lett 41:2606–2613

Su CH et al (2018) BARRA v1.0: the bureau of meteorology atmospheric high-resolution regional reanalysis for Australia. Geosci Model Dev Discuss 2018:1–33

Syktus JI, McAlpine C (2016) More than carbon sequestration: biophysical climate benefits of restored savanna woodlands. Sci Rep 6:29194

Taylor KE, Stouffer RJ, Meehl GA (2012) An overview of CMIP5 and the experiment design. Bull Am Meteorol Soc 93:485–498

Thatcher M, McGregor JL (2011) A technique for dynamically downscaling daily-averaged GCM datasets using the conformal cubic atmospheric model. Mon Weather Rev 139:79–95

Torma C, Giorgi F, Coppola E (2015) Added value of regional climate modeling over areas characterized by complex terrain—precipitation over the Alps. J Geophys Res Atmos 120:3957–3972

van Vuuren D et al (2011) The representative concentration pathways: an overview. Clim Change 109:5–31

Wong K, Syktus JI, Jeffrey S, Toombs N, Rotstayn L (2011) Climate extremes during the 20th and 21st centuries simulated by the CSIRO Mk3.6 climate model with anthropogenic and natural forcings. Modelling & Simulation Society of Australia & New Zealand, Perth